Electrical Power and Energy Systems 154 (2023) 109468

Contents lists available at ScienceDirect

International Journal of Electrical Power and Energy Systems

journal homepage: www.elsevier.com/locate/ijepes

Island detection for grid connected photovoltaic distributed generations via integrated signal processing and machine learning approach

Younis M. Nsaif [a,b], M.S. Hossain Lipu [c,*], Aini Hussain [a,d,*], Afida Ayob [a,d], Yushaizad Yusof [a,d]

[a] Department of Electrical, Electronic and Systems Engineering, Universiti Kebangsaan Malaysia, Bangi 43600, Malaysia
[b] General Company of Electricity Production, Middle Region, Iraqi Ministry of Electricity, Al Rusafa, Baghdad 10045, Iraq
[c] Department of Electrical and Electronic Engineering, Green University of Bangladesh, Narayanganj 1461, Dhaka, Bangladesh
[d] Centre for Integrated Systems Engineering and Advanced Technologies (INTEGRA), Universiti Kebangsaan Malaysia, Bangi 43600, Malaysia

ARTICLE INFO

Keywords:
Island detection
Distributed generation
Fault detection
Variational mode decomposition
Ensemble bagged trees method

ABSTRACT

The applications of distributed generators in distribution networks have proven to be highly reliable and cost-effective. Accidental islanding is currently regarded as an undesirable operational mode in utility practice because it can harm individuals and connected systems. Therefore, the occurrence of islanding must be detected, and then distributed generators must be disconnected from the main network. In this article, a fast and accurate island detection method is proposed for photovoltaic distributed generations with a near-zero non-detection zone. A new island detection approach is developed by combining signal processing and machine learning techniques. Variational mode decomposition is used as a signal processing technique. Whereas the ensemble bagged-trees method is used as a machine learning technique. Variational mode decomposition is used to process positive- and negative-sequence component voltage signals along with power signal measurements acquired from the point of common coupling in order to identify intrinsic-mode functions. Next, the ensemble bagged-trees method is utilized to detect islanding during active and reactive power mismatch events and inconvenient quality factors. The results demonstrate that the suggested technique is able to discriminate between islanding and non-islanding events such as capacitive switching, fault emulation, and distribution generation cut-off. Besides, it has a minimum non-detection zone of less than 4% and a 4.8 ms detection time. Therefore, it is a reliable and reasonable solution for the distribution grid.

1. Introduction

Recently, renewable distributed generation (DG) has gained attention for reducing transmission losses, mitigating distribution network congestion, and preventing global warming. Although the above reasons are important, several protection concerns are still related to distribution network integration with DGs [1]. One of these concerns is known as the islanding condition, which is described as a condition in which a section of the power system is comprised of distributed generation units, and loads are disconnected from the utility grid but remain energized [2]. Island events cause power system and DG malfunctions in the isolated section. Accordingly, the islanding event must be identified quickly within 2 s as per IEEE Standard 1547-2003 [3], and DG must be disconnected for reliable and safe distribution grid operation [4]. The island detection techniques can be classified into local and communication-based detection techniques. In general, local detection approaches can be divided into three types: passive, active, and hybrid-based detection approaches [5]. Therefore, an adequate island-detecting technology needs to be developed.

Numerous methods have been presented to detect an islanding condition. Before analysing these methods, it is necessary to highlight two crucial factors in order to comprehend the islanding phenomenon. The first factor is called the Non-Detection Zone (NDZ) criterion. NDZ is known as an active zone when the phenomenon of islanding cannot be identified on time, especially because of a small active/reactive power mismatch between generation and consumption in this zone [6]. The

Abbreviations: DG, Distributed generation; EBTM, Ensemble bagged-trees method; IMFs, Intrinsic-mode functions; NDZ, Non-detection zone; PCC, Point of common coupling; PMU, Phasor measurement unit; RUS, Random under-sampling; SNOP, Soft of normally open; SVM, Support vector machine; VMD, Variational mode decomposition.

* Corresponding authors at: Department of Electrical, Electronic and Systems Engineering, Universiti Kebangsaan Malaysia, Bangi 43600, Malaysia (A. Hussain).
E-mail addresses: shahadat@eee.green.edu.bd (M.S. Hossain Lipu), draini@ukm.edu.my (A. Hussain).

https://doi.org/10.1016/j.ijepes.2023.109468
Received 23 April 2023; Received in revised form 31 July 2023; Accepted 24 August 2023
Available online 31 August 2023

NDZ, depending on the island-detecting technology, is installed, and the threshold values are set. The second factor relates to the characteristics of the loads (located within the islanding area) that can be modelled by a parallel RLC circuit. The primary application of this circuit is for executing islanding analysis, as it creates an extremely challenging scenario for detecting islanding using relevant methods. The quality factor is a crucial factor in determining the reliability and robustness of the island detection method. The quality factor is inversely proportional to the power factor of the distribution network [7]. The quality factor impacts the size of the NDZ and the accuracy of detection [8]; thus, the performance analysis of the island detection methods is highly dependent on both NDZ and quality factor.

Communication-based detection techniques do not rely primarily on measurements of local variables in order to identify an island event. These techniques provide advantages over local detection approaches, such as high efficiency and small NDZ. Over time, several communication-based detection techniques have been developed to detect island. Meanwhile, the phasor measurement unit (PMU) was used by Radhakrishnan et al. [9] to obtain data including voltage, phase angle, frequency, and rate of frequency change. Then, the island is identified using a combination of principal component analysis with a sliding window and a mathematical morphological filter. Subramanian and Loganathan [10] also proposed an island detection technique based on a micro-phasor measurement unit. This technique has the advantage of distinguishing island from non-island events. Katyara et al. [11] used a phasor measurement unit, a wireless network, and voltage stability analysis to identify islands. Chafi et al. [12] proposed island detection based on monitoring the differences between voltage and current phasors at each DG acquired by micro-PMU. These differences are close to zero during normal operational conditions. Islanding happens when the differences exceed the threshold values. This technique can detect islanding within 0.12 s. Furthermore, the micro-phasor measurement unit and Fortescue transform are used by the authors in [13]. The sequence angle is determined by applying the Fortescue transform to voltage measurements obtained by a phasor measurement unit. The auhtors also used the angle difference between the positive and the negative sequence components for island detection. This technique is able to detect island within only 10 ms. Due to the utilisation of high-speed connections, cost is the only limitation of communication-based detection techniques.

The basis of active island detection techniques is injecting a disturbance into the distribution system to alter system parameters. In order to enhance islanding detection, many active-based methods have been established, such as irregular current injection [14], direct-axis current injection [15], direct-axis current injection with hybrid analysing approach [16], the ratio between direct-axis component of voltage at point of common coupling (PCC) and direct-axis current injection [17], frequency injection [18], three-phase current injection [19], active - frequency drift [20], active frequency drift with hyperbolic sine method [21]. However, active methods deteriorate power quality on the distribution grid, which might cause instability with the high integration of DGs. The passive-based detection method depends on continual monitoring and measurement of local data from PCC or DG terminals, including voltage, current, power, frequency, harmonic distortion, and phase angle. The island is identified by methodically comparing the variation of these variables to a set of threshold values. Under this category, over/under voltage, over/under frequency [5], rate of change of frequency [22], and harmonic distortion [6] studies have been proposed by researchers. Nevertheless, the main drawbacks of the passive technique are a larger non-detection zone and the necessity for proper threshold values. The hybrid method combines the best features of both passive- and active-based methods while eliminating their drawbacks [23]. Shrivastava et al. [24] proposed a hybrid island detection technique based on wavelet energy entropy recognition and an active frequency drift approach First-level wavelet energy entropy identified islanding based on the threshold value and activated the second-level approach. The second level utilized an active frequency drift approach integrated with a positive feedback pulsating fraction. The total time consumed by this technique is 0.32 s. The two-level island detection method is presented by Bakhshi-Jafarabadi et al. using the rate of change of voltage and active power signals [25]. This technique has the ability to discriminate between island and non-island events. In addition, this technique can detect island in less than 0.51 s. Serrano-Fontova and Bakhshi-Jafarabadi proposed a two-level island detection method based on the rate of change of frequency and threshold values [26]. Nevertheless, several techniques do not consider a DG cut-in event. Recently, researchers hybridize the island detection methods with intelligent data-based methods due to their adaptability and auto-tuning.

Numerous island techniques have been established with the advent of artificial intelligence, pattern recognition, and signal processing techniques. In [27], an adaptive neuro-fuzzy inference system has been presented to detect islanding for inverter-interfaced distribution grid. This technique has no negative impact on power quality. Low accuracy and a large NDZ are limitations of the approach. In the meantime, Shahryari et al. [28] proposed an island detection method based on the wavelet transform and neural networks. The wavelet transform is used to calculate the energy of time and frequency signals. Then, these signals are used to train and test neural networks in order to detect islands. The small NDZ of this method, which is around 6%, is one of its main advantages. However, this method was not tested within multiple DGs. Sadoughi, Hojjat, and Hosseini Abardeh [29] utilized a genetic algorithm to optimally select support vector machine (SVM) local input variables based on island detection time and error Then, SVM classification was trained and tested using these variables to detect islanding events. In another work [30], an anti-islanding technique based on a support vector machine is proposed. Here, seven signals were employed to detect the islanding condition: frequency, active power, reactive power, total harmonic distortion, and root mean square. After that, the SVM was trained and tested using these signals. This technique maintains good island detection time and superior accuracy. However, it has a large NDZ. Allan and Morsi [31] proposed a combination technique of continuous wavelet transform and deep learning technique for island detection. The continuous wavelet transforms extracted 31 features from the local system measurements. Then, the magnitudes of the coefficients obtained by the scalogram are used as input data for the deep learning technique. This technique can detect islanding within 2 s. The summary of the existing studies and research gaps are presented in Table 1. As shown in Table 1, a few of the existing techniques have

Table 1
Objectives and research gaps of the existing literature.

Ref.	Objectives	Research gaps
[25]	Detect islanding in 510 ms, and reasonable	Does not consider DG cut-in event.
[26]	Detect islanding within 473 ms, low computational complexity, reasonable, and zero NDZ	Does not consider DG cut-in event and load quality factor, and has no multi-DGs testing (i.e., solar photovoltaic DGs).
[28]	Near to zero NDZ, and the needless threshold value	Does not consider DG cut-in event, has no multi-DGs testing, and NDZ can be reduced.
[22]	Discriminate between islanding and non-islanding events, low detection time within 43 ms	Does not consider DG cut-in event, and has large NDZ.
[10]	Detect islanding in less than 14 ms, high accuracy and zero NDZ	Expensive, and does not consider DG cut-in event and load quality factor.
[9]	Detect islanding in 0.27 to 1.27 s, high accuracy and zero NDZ	Expensive, and detection time can be improved
[31]	Detect islanding in 0.21 s, High accuracy, and zero NDZ	Does not consider DG cut-in event and load quality factor, has no multi-DGs testing and detection time can be improved.

considered the effect of multi-DGs. Furthermore, only the technique in [9] considered DG cut-in events. Only four methods have considered the load quality factor in assessing island detection performance. While some techniques offered zero NDZ. However, there is a need to detect islanding quickly, accurately (during DG cut-in event and inconvenient load quality factors) and cost-effectively with high accuracy in multi-DGs.

To bridge the above research limitations, the integration of signal processing and machine learning techniques is proposed in this paper to detect islanding in distribution grids. Local measurements of both voltage and power signals taken from PCC are processed using variational mode decomposition (VMD) to identify intrinsic-mode functions. Inadequately defined threshold values significantly affect detection time and accuracy. Therefore, the proposed technique uses machine learning to overcome the drawbacks of threshold values. The authors used a supervised machine learning technique called the ensemble bagged-trees method to improve the accuracy of island detection. The key innovations of the proposed technique are underlined, including:

- The proposed method has been able to detect islanding in a low-voltage distribution grid when the active/reactive power mismatch is close to zero and achieves the minimum NDZ.
- The proposed strategy has been demonstrated to be capable of discriminating between island (i.e., active and reactive power mismatch events and inconvenient quality factors) and non-island events, including capacitive switching, DG cut-in events, and fault emulation.
- A new local-based island detection strategy utilizing VMD and the ensemble bagged-trees method (EBTM), where VMD is used to deal with non-stationary signals. Additionally, the outcomes of EBTM are compared with four traditional machine learning techniques, which are trained and tested using the same data as EBTM. It is found that the suggested EBTM can detect islands efficiently and accurately.

This paper consists of five sections. Section 2 introduces the proposed island detection methodology. The investigated test system is shown in section 3. Results and discussions are highlighted in Section 4. Finally, Section 5 discusses the conclusions.

2. Proposed island detection methodology

This section outlines the presented technique in detail. VMD is utilized to acquire unique features from positive-, and negative-sequence component voltage signals along with three-phase power signals. Subsequently, the island is achieved by using EBTM.

2.1. Variational mode decomposition

VMD is applied to obtain the prominent features in the time–frequency domain, that have multiple benefits, such as being self-adaptive, noise-resistant, and having no effect on mode mixing. Multi-component signal decomposition, identification of sidebands, extraction of intra-wave characteristics, and noise robustness are all fields where the VMD surpasses the empirical-mode decomposition. Therefore, features of the signal were extracted using VMD instead of empirical-mode decomposition.

Decomposing a signal into sub-signals known as intrinsic-mode functions (IMFs), VMD is an adaptive signal processing method that is non-recursive, and fully intrinsic. The VMD technique divides the signal $Y(t)$ into a defined number of IMFs. Every IMF possesses bandwidth limitations [32]. Input signals can be reproduced using the decomposed modes, which have a unique sparsity property. The IMFs are constructed using a sine waveform function.

$$Y_k(t) = \sum_{k=1}^{K} M_k(t)\cos\theta_k(t) \tag{1}$$

where K represents the modes level, $Y_k(t)$ denotes IMFs, and $M_k(t)$ indicates a positive envelope of IMFs. Furthermore, $\theta_k(t)$ denotes the non-decreasing phase angle. The preponderance of every mode rotates around the fundamental frequency. Furthermore, an IMF is a reproduction of a significant disruption in the original signal at various amplitudes. The input signal $f(t)$ can be recovered by a combination of IMFs. The centre frequency and bandwidth of every specified IMF can be determined by applying a stable optimization method to improve the optimum variational problem solution [33]. The decomposition problem for every signal can be expressed as:

$$\begin{aligned} L(\{M_k\},\{w_k\},\lambda) = \alpha\sum_k \left\| \frac{d}{dt}\left[\left(\delta(t)+\frac{j}{\pi t}\right)*M_k(t)\right]e^{-jw_k t}\right\|_2^2 \\ + \left\| f(t) - \sum_k M_k(t)\right\|_2^2 \\ + \left\langle \lambda(t), f(t) - \sum_k M_k(t)\right\rangle \end{aligned} \tag{2}$$

where w_k represents the central-angular-frequency, and δ denotes the Dirac-distribution. Moreover, * indicates the convolution. j represents the imaginary part where the value $j^2 = -1$. Additionally, α denotes the quadratic penalty term, and λ denotes Lagrangian-multiplier. Eq. (2) can be effectively minimised using a multiplication approach based on alternating directions. The updated values for the centre frequency and the evaluated modes in the frequency response are shown below.

$$\widehat{M}_k^{n+1}(w) = \frac{\widehat{f}(w) - \sum_{i<k}\widehat{M}_i^{n+1}(w) - \sum_{i>k}\widehat{M}_i^{n}(w) + \frac{\widehat{\lambda}(w)}{2}}{1+2\alpha(w-w_k)^2} \tag{3}$$

$$\sum_k \frac{\left\|\widehat{M}_k^{n+1} - \widehat{M}_k^{n}\right\|_2^2}{\left\|\widehat{M}_k^{n}\right\|_2^2} < \varepsilon \tag{4}$$

The mathematical procedure for updating the modes and their center frequencies depending on the number of selected modes (n) is expressed in Eqs. (3) and (4), where $\widehat{M}_k^{n+1}(w)$ and w_k^{n+1} represent the amplitude and centre-frequency of $(n+1)$ the next mode in the kth level, respectively. $\widehat{f}$ represents the Fourier transform of f. ε indicates an adequate tolerance rate. A new Lagrangian-multiplier is calculated as,

$$\widehat{\lambda}_{n+1}(w) = \widehat{\lambda}_n(w) + \tau\left(\widehat{f}(w) - \sum_k \widehat{M}_k^{n+1}(w)\right) \tag{5}$$

where τ denotes the Lagrangian-multiplier update rate. As the number of iterations increases, the algorithm, central frequencies, and Lagrangian-multiplier continue to update the modes until convergence is reached.

2.2. Sliding-window analysis technique

A sliding-window analysis technique is typically used in order to preserve the real-time features of the signals before extracting islanding characteristics. VMD requires the length of the signal to be specified to ensure proper IMF output. The sliding-window analysis technique is utilised in the suggested strategy to mitigate the impact of data preparation. In this technique, a sample of a specified size is obtained by sliding a window of known length under a given time window. By sliding the sample through time, the sample is continuously updated. Some new data arrives after a predetermined interval of time and the old data of the same interval in the past are discarded. A new sample of fixed length is produced [34]. The required data for VMD could be created speedily

using this technique. Conversely, the size of the sliding window has a direct impact on the efficiency of the technique.

2.3. Ensemble-bagged-trees method

Machine learning techniques are categorized into three distinct types: supervised, semi-supervised, and unsupervised. One of the most widespread classification techniques is supervised machine learning. Training errors are employed in the training function to acquire classification capabilities. The use of this closed-loop feedback could improve the efficacy of machine learning technique classification [33]. In this study, the basic learner for EBTM was built using supervised machine learning techniques.

Ensemble learning methodology can be implemented in three main stages. The flow diagram of the EBTM is illustrated in Fig. 1. The initial step involves adapting training data sets. The training data sets are partitioned into subsets and each sample dataset in a subset could be selected many times. Where n represents a randomly selected subset from the full training dataset. The second stage involves the selection of predictive models. In the final stage, known as the member combining stage, predictions from various classifiers are combined. Designers use average, weighted-average, majority-voting, and weighted-majority voting to combine the outputs of multiple classifiers into one final prediction using an ensemble technique. Ensemble learning algorithms like bagging, random subspace, and boosting are commonly used to establish machine learning classifiers. In this study, the EBTM was presented as a solution to the classification issue between islanding and non-islanding events.

Bagging, or bootstrapping aggregation, is a common statistical technique. Utilising bagging has multiple benefits. First, by generating numerous classifiers with a constant bias and then averaging the results, both variance and model overfitting are reduced [35]. This method is very effective when entry characteristics are extremely variable and the bias level is minimal. Secondly, bagging creates several boot-strap sets from the training dataset, trains the dataset with a classifier, and aggregates the outputs of every model with a practical approach, for instance, majority-voting.

2.4. Island detection algorithm

The overall flow chart of the suggested island detection algorithm employing VMD and EBTM is depicted in Fig. 2. The algorithm starts by acquiring three-phase voltage and current from PCC. After that, the positive-, and negative-sequence components of a three-phase voltage signal can be determined with the use of a sequence analyser. Simultaneously, the three-phase active power is computed by utilising voltage and current data. The active power, positive-, and negative-sequence component signals are all subjected to a sliding window mechanism after selecting an appropriate window size. Then, VMD is applied to acquire IMFs mode-3 of the three signals individually. Finally, EBTM is utilized to differentiate islanding from non-islanding events.

3. Investigated test system

The suggested island detection algorithm has been tested in multiple

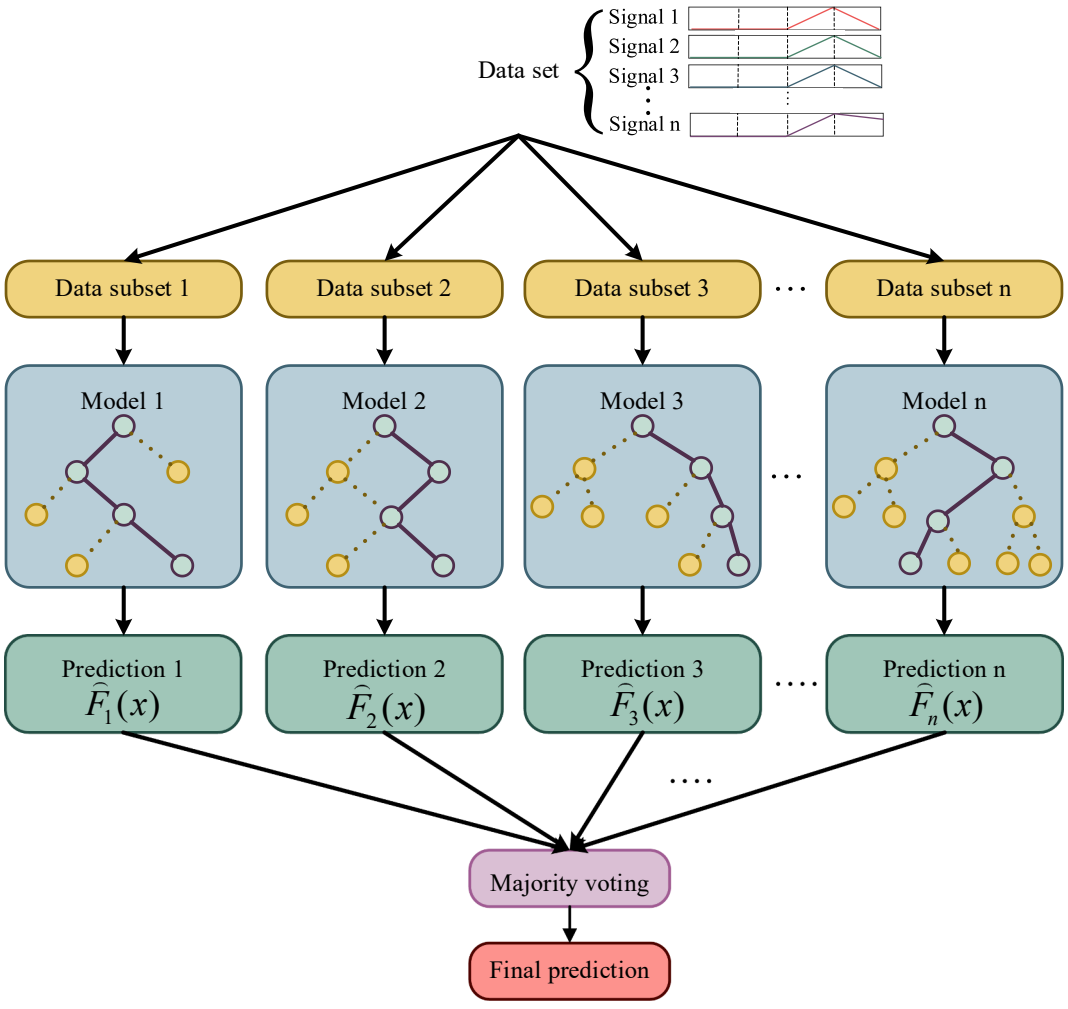

Fig. 1. The flow diagram of the EBTM.

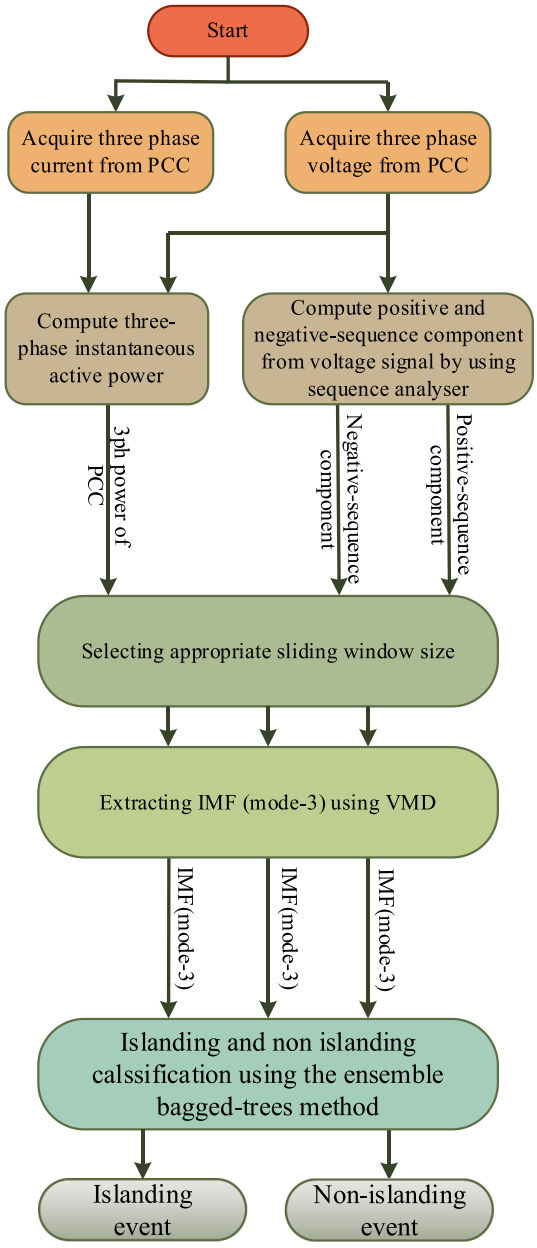

Fig. 2. The overall flow chart of the suggested island detection algorithm.

scenarios. The test system evaluated in this article is a modified part of an existing Malaysian distribution grid, as illustrated in Fig. 3. The distribution network is comprised of grid utility, with 20 lumped loads and 23 buses. Furthermore, the part of the modified island test system comprised two photovoltaic panels, two battery banks, two inverters, two PCC (PCC-1 and PCC-2), six busbars and three loads (Load 1, Load 2, and Load 3) as demonstrated in Fig. 4.

Two inverter-interfaced distribution generations are powered by the distribution network along with the grid utility. The modified Malaysian distribution network generation provides the load data as presented in Table 2. In addition, the components of the island testing system and their specifications are listed in Table 3. The island distribution network comprises two step-down transformers of 11 kV/0.4 kV where transformer one (TR1) is placed between busbar 1 (bus1) and busbar 3 (bus3). Transformer two (TR2) is located between busbar 2 (bus 2) and busbar 4 (Bus 4). A soft normally open point-circuit breaker (SNOP-CB) is employed to change the distribution network topology from radial to mesh and vice versa. Simulating islanding is achieved by opening the circuit breaker (CB5). The effectiveness of an island detection method can vary depending on the type of load. A parallel RLC circuit can be used to simulate this type of load, as defined by the IEEE 1547 test frame. This circuit is mainly used because it presents a greater challenge for island detection methods than alternative circuits.

R, L, and C values for the unity power factor load can be calculated as follows [37]:

$$R = \frac{V^2}{P} \tag{6}$$

$$L = \frac{V^2}{2 \times \pi \times f \times Q_f \times P} \tag{7}$$

$$C = \frac{Q_f \times P}{2 \times \pi \times f \times V^2} \tag{8}$$

where Q_f represents the quality factor, which is the ratio between the amount of energy stored in the reactive components of the load and the amount of energy dissipated through the load's resistance [36]. Nevertheless, the inductance (L) and capacitance (C) values can be computed in the situation of a non-unity power factor, using the formulas below:

$$X_L = \frac{V^2}{Q_L} \tag{9}$$

$$L = \frac{X_L}{2 \times \pi \times f} \tag{10}$$

$$X_C = \frac{V^2}{Q_c} \tag{11}$$

$$C = \frac{1}{2 \times \pi \times f \times X_C} \tag{12}$$

where X_L and X_C represent the inductive and capacitive reactance, respectively.

4. Results and discussion

Using VMD, the feature was extracted from active power, positive- and negative-sequence components of voltage. Different modes can be extracted by VMD. However, a high decomposition level is preferred to maximise signal feature reliability. Moreover, there are several drawbacks associated with a high decomposition level. The increased computing load caused by a larger number of modes can slow down the islanding detection method. Therefore, IMFs mode-3 was selected for implementing VMD. In this article, the MATLAB/Simulink environment was used to execute VMD. Accurate operation of VMD in MATLAB Simulink requires signal adaptation based on a sliding window. Both the sample size and the sampling frequency are vital. For the proposed sliding window technique to operate correctly, it is required to precisely specify the sample size. A sliding-window method with 2048 samples per window is being used to achieve a balance between the two competing requirements, minimal processing time and appropriate characteristic extraction. For discrete-simulation types, the sample time interval is described as 2.5×10^{-6} s. The proposed island detection method has been extensively tested in both islanding and non-islanding scenarios to validate its accuracy.

4.1. Islanding scenarios

In this sub-section, the islanding scenarios were outlined. The functionality of the proposed island detection technique in identifying islanding scenarios was validated in this study. The islanding scenarios, including both active and reactive power mismatches and quality factors, are taken into consideration in this article. Table 4 demonstrates

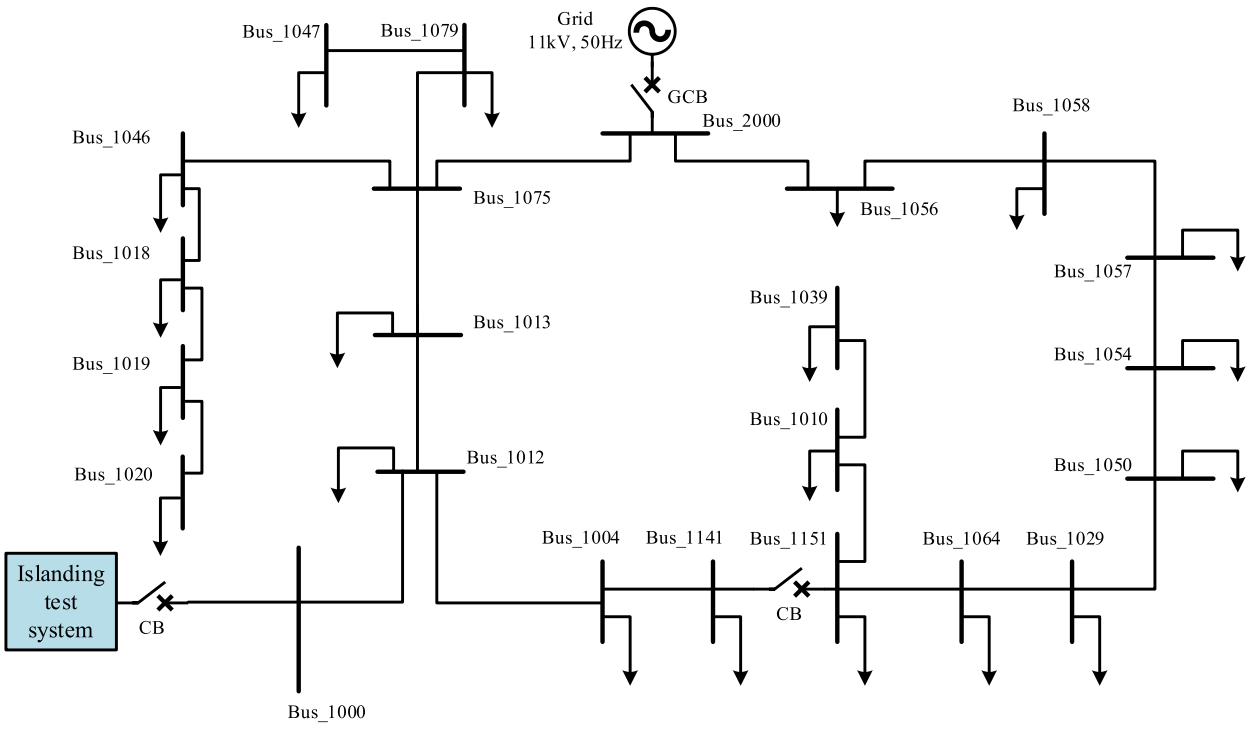

Fig. 3. 11 kV Malaysian distribution network [36].

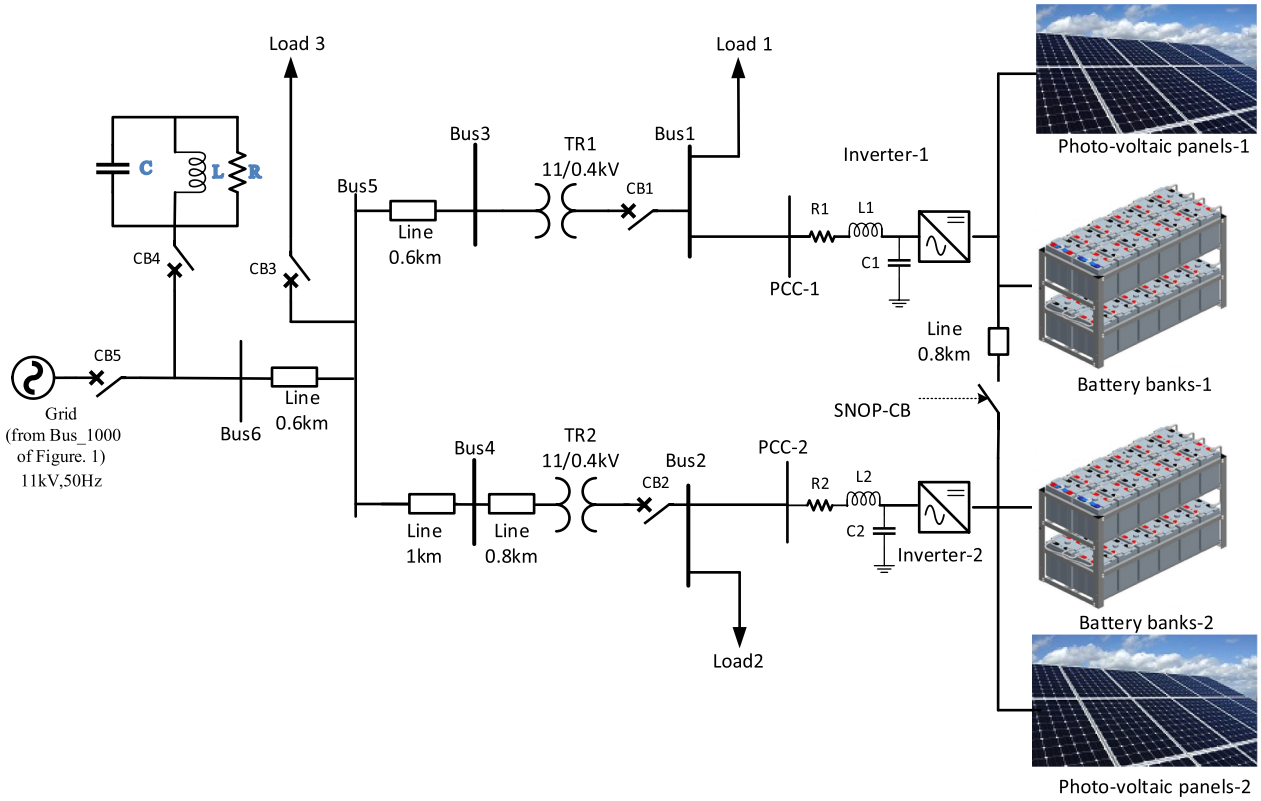

Fig. 4. Schematic diagram of the island test system.

the island scenarios under investigation.

4.1.1. Active and reactive power mismatch

The fluctuation of PCC voltage in the island region is heavily influenced by the number of active and reactive power mismatches. Therefore, the conventional island detection method fails to detect islanding when active and reactive power mismatches are close to zero. Consequently, the initial evaluation has been conducted in cases (1–24) for different $\Delta P + j\Delta Q$ during both radial and mesh-SNOP topologies of the distribution network. Islanding events during active and reactive

Table 2
Generation and load data of modified Malaysian distribution network.

Bus no.	Pg (Mw)	Qg (MVAr)	PL (MW)	QL (MVAr)
1	0.01193	0	0.005	0
2	0.01193	0	0.005	0
5	0	0	0.01	0
1013	0	0	0.07	0.05
1141	0	0	0.097	0.05
1012	0	0	0.1	0.05
1050	0	0	0.1095	0.05
1047	0	0	0.1179	0.05
1079	0	0	0.1	0.05
1057	0	0	0.189	0.09
1058	0	0	0.198	0.09
1010	0	0	0.1383	0.05
1039	0	0	0.1	0.05
1064	0	0	0.1488	0.05
1018	0	0	0.1743	0.09
1154	0	0	0.21	0.09
1004	0	0	0.2121	0.05
1046	0	0	0.2535	0.1
1020	0	0	0.2745	0.1
1029	0	0	0.3468	0.1
1019	0	0	0.191	0.05
1151	0	0	0.2218	0.05
1056	0	0	0.3475	0.1

Table 3
The island test system component specifications.

No.	Component	Specification
1	Photo-voltaic panels-1 and Photo-voltaic panels-2	2 Parallel strings, 28 series-connected modules per string, irradiance 1000 W/m2
2	Inverter-1 and inverter-2	12.5 kVA, 0.4 kV, 50 Hz, switching frequency 5 kHz Filter:- Series-Inductance (L1, and L2) 4.6 mH Series-Resistance (R1, and R2) 0.4596 Ω Shunt-Capacitance (C1, and C2) 0.1102 μF
3	Battery bank-1, and battery bank-2	Lead-Acid, 980 V, 12Ah
4	Transformer (TR1, and TR2)	11/0.4 kV,24kVA,50 Hz,D11/Yn
5	Load 1	5 kW, 0.4 kV,50 Hz
6	Load 2	5 kW, 0.4 kV,50 Hz
7	Load 3	10 kW, 11 kV, 50 Hz

mismatch in cases 3, and 9 are depicted in Figs. 5 and 6 correspondingly. Where the blue line indicates the IMF mode-3 of the positive-sequence voltage component waveform. Furthermore, the magenta line denotes the IMF mode-3 of the negative-sequence voltage component waveform. The green line represents the IMF mode 3 of the three-phase power signal. The IMFs of the positive-, and negative-sequence components of voltage waveform during the island of case 3 were considerably raised to 7.97 and 2.83, respectively. In the meantime, the IMF of the three-phase power signal was increased to 110.45. During the islanding of Case 9, both IMFs of the positive, and negative sequence voltage component waveforms were increased dramatically to 4.89 and 2.67, respectively. IMF of the power signal was raised to 46. Consequently, the proposed technique is capable of identifying islanding in this case.

4.1.2. Inconvenient quality factors

The performance of the suggested island detection method was evaluated by altering the quality factors according to IEEE 1547, UL1741, and IEEE 929 standards. IEEE 1547 standard recommends testing islanding with loads that have a quality factor of 1. The islanding event must be identified in under 2 s in order to satisfy the UL 1741 test for RLC loads with a quality factor $\leq$1.8. A quality factor of $\leq$2.5 is suggested by the IEEE 929 standard. The quality factor values used to determine the effectiveness of the produced island detection method take the recommendations of all three standards into account. Table 5

Table 4
The Islanding Scenarios Under Investigation.

Case No.	Description	ΔP + jΔQ(%)	Topology
1	Active and reactive power mismatches (open CB5)	−12	Radial
2		−8	
3		−4	
4		+4	
5		+8	
6		+12	
7		−12	Radial without battery banks
8		−8	
9		−4	
10		+4	
11		+8	
12		+12	
13		−12	Mesh-SNOP
14		−8	
15		−4	
16		+4	
17		+8	
18		+12	
19		−12	Mesh-SNOP without battery banks
20		−8	
21		−4	
22		+4	
23		+8	
24		+12	
25	1.8 quality factor	–	Radial
26	2.5 quality factor	–	
27	3 quality factor	–	
28	1.8 quality factor	–	Mesh-SNOP
29	2.5 quality factor	–	
30	3 quality factor	–	

depicts the R, L, and C values that relate to the various quality factor values. IMFs mode-3 extracted from positive, and negative sequence components of the voltage signal are displayed in Fig. 7 (a and b). The IMFs mode-3 obtained from the power signal is depicted in Fig. 7 c. The IMFs signals during the quality factor of 1.8, 2.5, and 3 are denoted in blue, red, and green colours, respectively. It has been noticed that IMF mode-3 of the positive-sequence component of the voltage signal reached the highest level during the quality factor equal to 1.8 as compared with 2.5, and 3. The IMF mode-3 of the negative-sequence component of the voltage signal reaches its maximum level at a quality factor of 2.5. Correspondingly, the IMF mode-3 of the power signal attains its highest level at a quality factor of 2.5.

4.2. Non-Islanding scenarios

Regardless of an efficient island detection method, the proposed technique must not exhibit unwanted tripping in non-islanding scenarios. The non-islanding scenarios investigated in this study are depicted in Table 6, where different levels of capacitive bank switching, DG cut-in events, and fault emulation are included in non-islanding scenarios. Moreover, normal events during both radial and mesh-SNOP are considered in non-islanding scenarios.

4.2.1. Capacitive bank switching

When the capacitor banks are linked in parallel with the load to improve the voltage sag and the power factor, the passive parts of the system are altered. To evaluate the performance of the module as the passive parameters change, the capacitor bank ratings used in this scenario, including (1.4, 0.9, and 0.5 MVAr), are switched at 0.2 s. Fig. 8 is shown the VMD IMF_3 variation during the capacitor bank switching in case 32. Here, the IMF mode-3 of the positive-sequence component of the voltage signal is achieved 0.0013. In the meantime, the IMF mode-3 of the negative-sequence component of the voltage signal is raised to 0.74. The IMF mode-3 of the power signal is reduced to 0.00038. This shows that the suggested island detection method can accurately

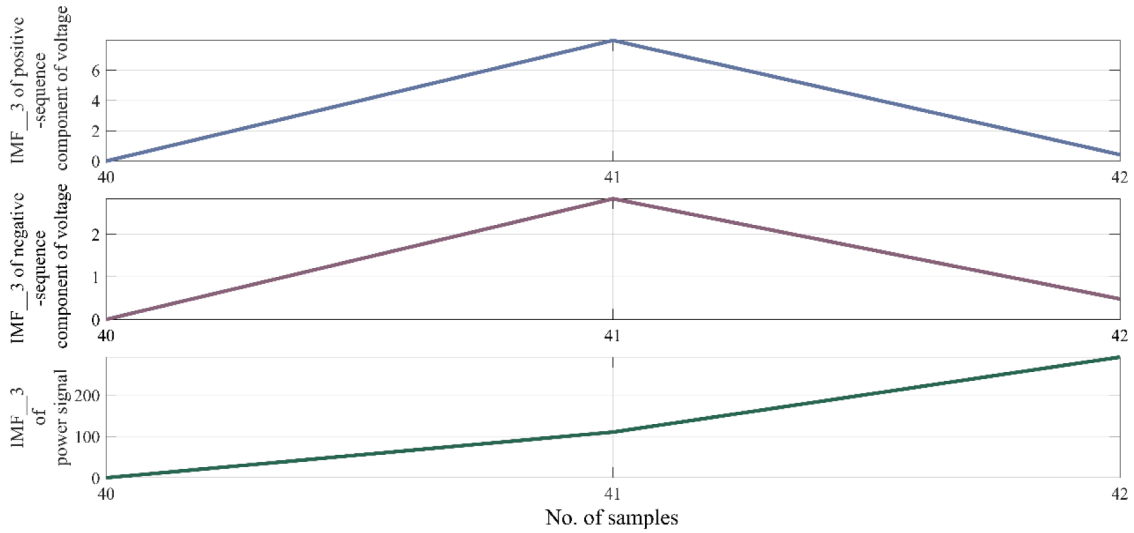

Fig. 5. Island event owing to active and reactive power mismatch case 3.

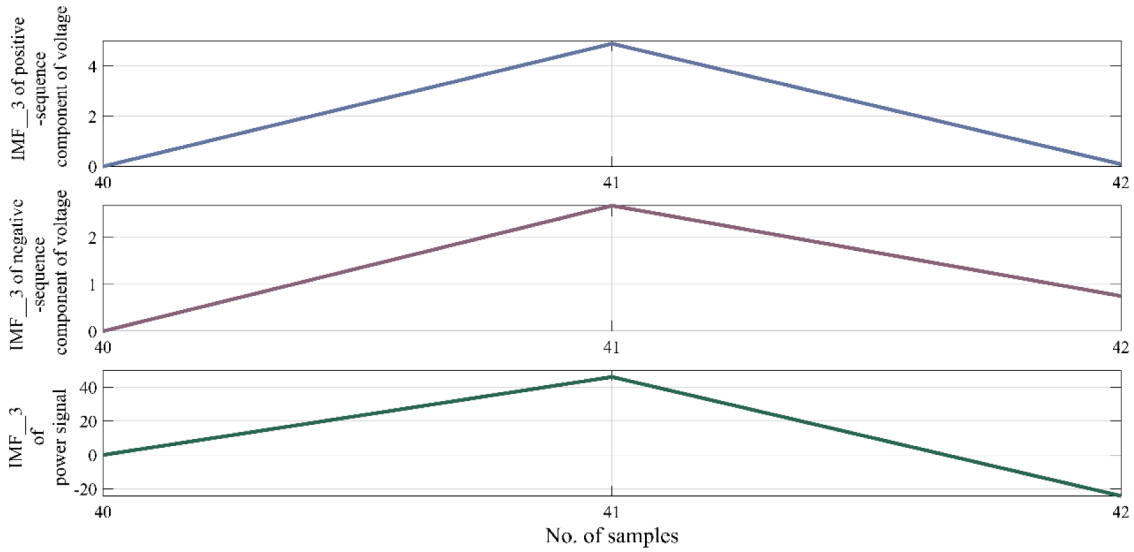

Fig. 6. Island event owing to active and reactive power mismatch case 9.

Table 5
The resistance, inductance, and capacitance values for different quality factors.

Quality factor	Resistance (Ω)	Inductance (H)	Capacitance (F)
1.8	2.304	0.00304	0.00196
2.5	2.304	0.00244	0.002873
3	2.304	0.00203	0.003442

identify capacitor bank switching as a non-islanding scenario.

4.2.2. Distributed generation cut-in event

A DG cut-in scenario was conducted to extensively evaluate the performance of the suggested technique. In order to simulate a DG cut-in event, inverter interface DG 2 is disconnected from the distribution network at 0.2 s. Fig. 9 depicts VMD IMF_3 response to DG cut-in event in case 35. Here, IMF mode-3 of positive-sequence component of the voltage signal reaches to 0.2×10^{-4}. IMF mode-3 of negative-sequence component of the voltage signal decrease to 0.5×10^{-3}. The IMF mode-3 of the power signal increases to 14.99×10^{-3}. By conducting a comparative analysis between the IMF mode-3 values observed during the DG cut-in event and the IMF mode-3 values observed during islanding events shown in Figs. 5, 6, and 7, it can be noticed that the IMF mode-3 of positive-sequence and negative-sequence components of the voltage signal, and the power signal are considerably lower during DG cut-in event. Consequently, the suggested technique differentiates between the DG cut-in events and islanding conditions.

4.2.3. Fault emulation

One of the critical concerns in power systems that could lead to ineffective anti-islanding methods are fault events. In addition, the main purpose of this analysis is to evaluate the performance of the suggested island detection technique in inherently imbalanced situations. Thus, fault events in different distribution network topologies are also considered in this article. Symmetrical and asymmetrical faults are initiated in the distribution network to assess the efficiency of this method. Fig. 10 illustrates the VMD IMF_3 response to the faulty event during case 38. It can be easily discovered that the IMFs of the positive, and negative sequence voltage component waveforms were raised slightly to 0.69 and 1.09, respectively whereas the IMF of the three-phase power signal started to gradually increase to 0.9 at sample number 41. When comparing the IMF mode-3 values acquired during

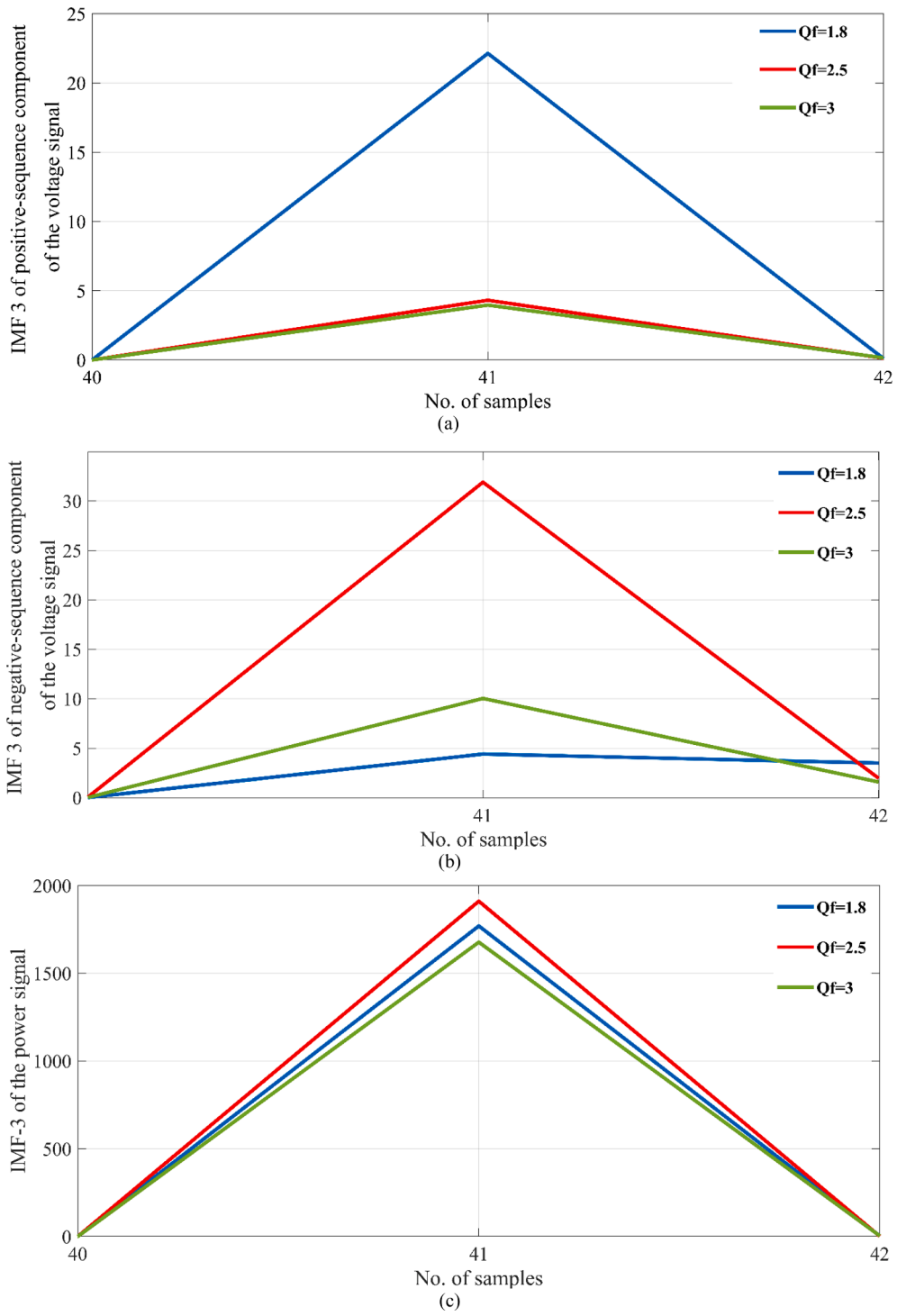

Fig. 7. Variation of VMD IMF_3 during various quality factors (a) IMF_3 of the positive sequence component of the voltage signal, (b) IMF_3 of the negative sequence component of the voltage signal, and (c) IMF_3 of the power signal.

islanding events shown in Figs. 5, 6, and 7 to the IMF mode-3 values during the fault event shown in Fig. 10, it is clear that the IMF mode-3 values for the positive-sequence and negative-sequence components of the voltage signal and the power signal are significantly lower during the fault event. Therefore, the suggested method identifies these cases as non-islanding conditions, allowing normal system operation.

4.3. Performance verification of machine learning techniques

The efficiency of four conventional machine learning techniques is compared with EBTM in this section. Table 7 presents the results obtained with five machine learning techniques. A total of 62 island and non-island cases have been used to test the capabilities of machine learning techniques. Ensemble random under-sampling (RUS)-boosted trees has been observed to acquire the lowest accuracy rate, while the accuracy rates of linear discriminant, cosine k-nearest neighbors (KNN), and linear SVM techniques are 72.6, 82.3, 87.1% respectively. Conversely, it has been found that EBTM can acquire superb accuracy. Fig. 11 depicts the performance of five machine learning techniques based on F1-score, precision, recall, and accuracy metrics. It is clear that

Table 6
The Non-islanding scenarios under Investigation.

Case No.	Description	Load	Topology
31	Normal	Balance	Radial
32	Capacitive bank switching	1.4 MVAR	
33		0.9 MVAR	
34		0.5 MVAR	
35	DG cut-in event (open CB2)	–	
36–46	Fault (SLG, LL, LLL,3LG) near to bus-21	–	
47	Normal	Balance	Mesh-SNOP
48	Capacitive bank switching	1.4 MVAR	
49		0.9 MVAR	
50		0.5 MVAR	
51	DG cut-in event (open CB2)	–	
52–62	Fault (SLG, LL, LLL,3LG) near to bus-21	–	

EBTM is outstanding to the other four machine learning techniques based on F1-score, precision, recall, and accuracy metrics. Therefore, EBTM is chosen to detect islanding events. Lastly, both VMD, and EBTM techniques were applied to obtain the island detection time in MATLAB/Simulink. Accordingly, an islanding event could be identified in only 4.8 ms with the proposed island detection method.

4.4. Comparison with related techniques

Various existing island detection methods that have been published were chosen for comparison. Table 8 provides a detailed comparative study between the proposed island technique and several existing techniques. The aspects included in this comparison are NDZ, quality factor, accuracy, and detection time. The phenomenon of islanding was observed within 90 ms using the technique established by [37]. Shahryari et al. observed the occurrence of islanding within 50 ms [28]. Song et al. identified islanding within 40 ms [38]. While, Tajdinian et al. observed the occurrence of islanding within a time range of 43–27 ms [22]. Islanding can be detected with zero NDZ and 10 ms detection time using the technique established by [13]. Similarly, Nale et al. identified islanding with zero NDZ, but here it was detected within 0.503 s [39]. Both of these techniques are classified as communication-based techniques. However, the only limitation of communication-based techniques is their cost. In addition, the deep learning technique in [31] can also obtain zero NDZ. Nevertheless, Allan and Morsi do not take into account the impact of the quality factor. Baghaee et al. proposed a technique with a 0.04 s detection time and 100% accuracy [30]. But it has a large NDZ. The technique suggested by [40] possesses a detection

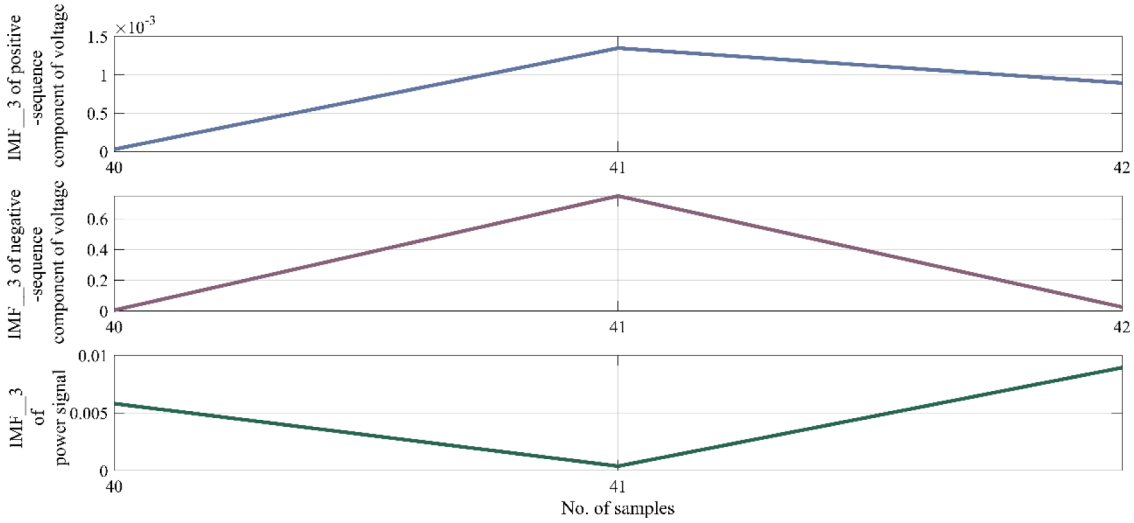

Fig. 8. Variation in VMD IMF_3 during the capacitor bank switching in case 32.

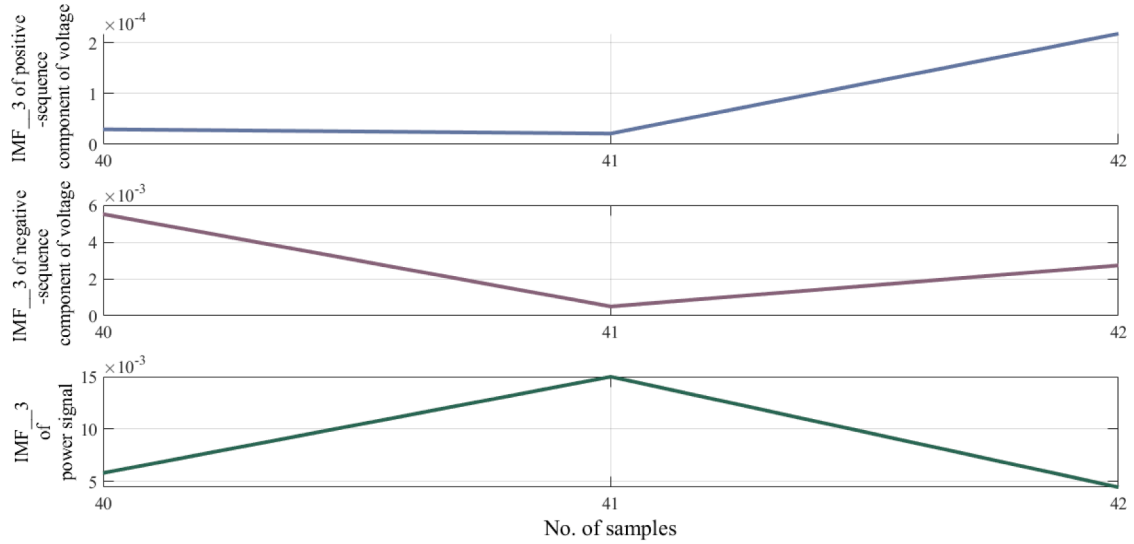

Fig. 9. VMD IMF_3 response to DG cut-in event in case 35.

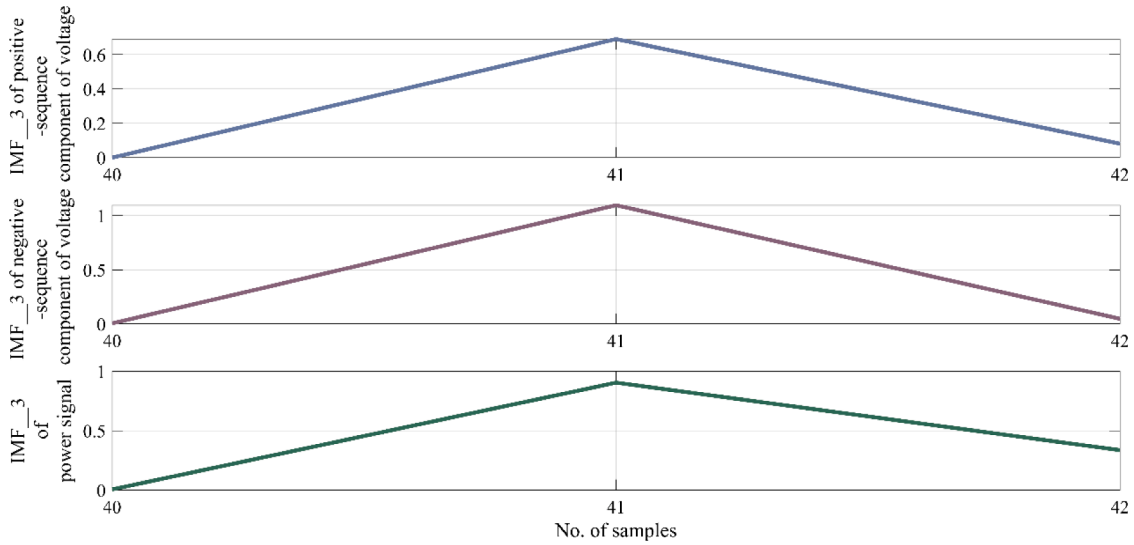

Fig. 10. VMD IMF_3 response to faulty event in case 38.

Table 7
The accuracy acquired by numerous machine learning techniques.

Technique	Accuracy	Cases	Validation methods
Ensemble RUS-Boosted trees	51.6%	62	Re-substitution validation
linear discriminant	72.6%	62	Re-substitution validation
Cosine KNN	82.3%	62	Re-substitution validation
linear SVM	87.1%	62	Re-substitution validation
EBTM	100%	62	Re-substitution validation

accuracy of 95–100% and a detection time of 10–20 s. However, it does not consider quality factor events. On the other hand, the proposed technique relies solely on local data taken from PCC and does not require any connection channels. In comparison to other methods in Table 8, the proposed method obtains considerably superior results regarding detection time and accuracy. Fig. 12 shows a comparative result between the proposed and existing local-based techniques in terms of NDZ, where, the techniques were selected based on the relevant features. It can be observed that the proposed technique possesses a minimum NDZ as compared to the technique in Fig. 12.

5. Conclusion

This paper proposes a new island detection method for photovoltaic distributed generation. Both the signal processing technique and the machine learning technique are used in the proposed method. Positive and negative sequence component voltage signals, as well as power signals, are processed with variational mode decomposition to acquire hidden features. Afterwards, the ensemble bagged-trees method is applied to detect islanding. This proposed method is then compared with four traditional machine learning techniques such as ensemble random under-sampling-boosted trees, linear discriminant, Cosine K-nearest-neighbours, and linear support vector machines. The ensemble bagged-trees method provides high performance in regards to F1-score, precision, recall, and accuracy metrics. Due to its reliance on local data, the proposed method is reasonable to implement. Based on extensive tests for a variety of events, the proposed technique is able to differentiate between islanding and non-islanding events such as capacitive switching, fault emulation, and distributed generation cut-in. In addition, the suggested method possesses a minimum non-detection zone. The proposed method is capable of detecting islanding during active and reactive power mismatch events and inconvenient quality factors in 4.8 ms. Therefore, the proposed technique offers a high degree of dependability.

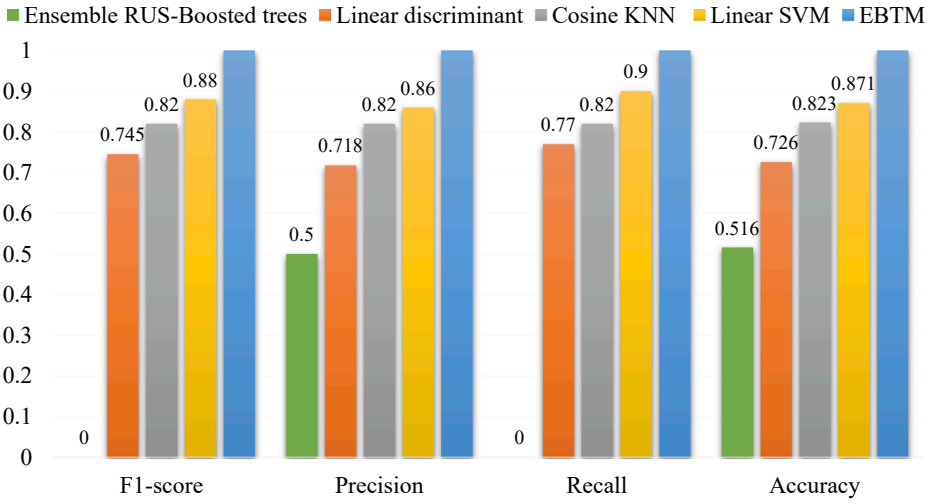

Fig. 11. The performance of five machine learning techniques based on F1-score, precision, recall, and accuracy metrics.

Table 8
Comparison of various existing island detection methods with the proposed methodology.

Ref.	Method	Variable	NDZ	Quality factor	Accuracy (%)	Detection time
[37]	Rate of change of active power, Rate of change of reactive power, and threshold values.	Voltage, current, active power, and reactive power	$-5\% \leqslant \frac{\Delta P}{P} \leqslant 4.3\%$, $-4.5\% \leqslant \frac{\Delta Q}{Q} \leqslant 4.3\%$	Yes	N/A	90 ms
[22]	Frequency, rate of change of frequency	Voltage	$-10\% \leqslant \frac{\Delta P}{P} \leqslant 10\%$ $-10\% \leqslant \frac{\Delta Q}{Q} \leqslant 10\%$	Yes	99.53	27–43 ms
[27]	Adaptive neuro-fuzzy inference system	Voltage, current, frequency, active and reactive power	49%	Yes	78.71	40 ms
[28]	Wavelet transform, and neural network	Voltage, and current signal	< 6%	Yes	<98	<0.05 s
[30]	Support vector machine,	RMS value of voltage, and current, threshold value of voltage and current, frequency, active and reactive power	9.52%	Yes	100	0.04 s
[13]	Micro phaser measurement unit, communication channels, Threshold values	Voltage, active power	Zero	No	N/A	10 ms
[40]	Decision tree	Voltage and current	Minimal NDZ	No	95–100	10–20 ms
[31]	Wavelet transform, deep learning	Single and three-phase voltage, and current,	Zero	No	98.6	0.21 s
[5]	Continuous wavelet transforms, and threshold values	Voltage, and current	N/A	No	N/A	0.16–2 s
[38]	Synchronous reference frame phase lock loop, Harmonic spectrum, virtual impedances, and threshold value	Voltage, current of inverters 1, and 2	N/A	N/A	N/A	≤2 s
[39]	Butterworth filter, weighted least error square technique, communication channel, superimposed impedance phase angle difference between DG and PCC	DG Voltage and current, PCC voltage and current	Zero	Yes	N/A	0.503 s
Proposed technique	VMD, and EBTM	Voltage and current	$-4\% \leqslant \frac{\Delta P}{P} + j\frac{\Delta Q}{Q} \leqslant 4\%$,	Yes	100	4.8 ms

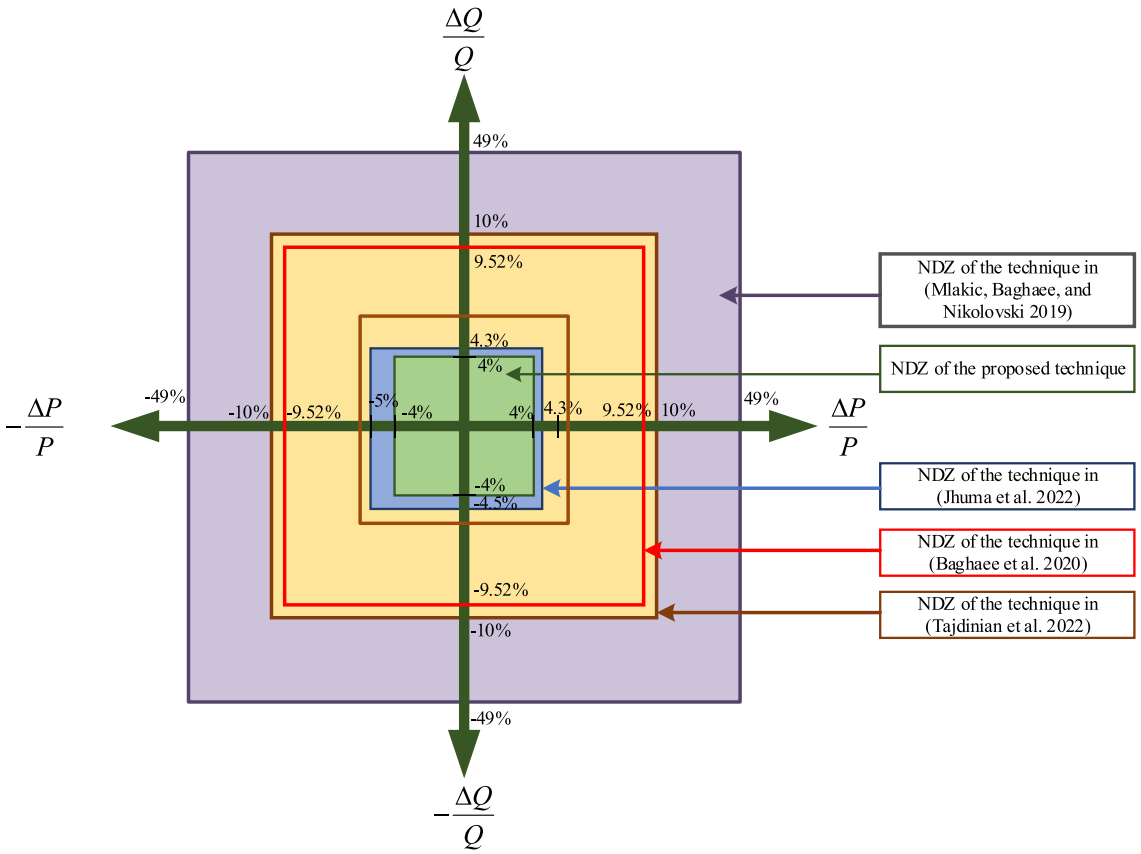

Fig. 12. Comparative results between the proposed and existing local-based techniques in terms of NDZ.

Finally, real-time verification of the suggested method in a hardware-in-the-loop system requires further research.

CRediT authorship contribution statement

Younis M. Nsaif: Conceptualization, Methodology, Software, Validation, Writing – original draft. **M.S. Hossain Lipu:** Supervision. **Aini Hussain:** Supervision, Project administration, Funding acquisition. **Afida Ayob:** Writing – review & editing. **Yushaizad Yusof:** Writing – review & editing.

Declaration of Competing Interest

The authors declare that they have no known competing financial interests or personal relationships that could have appeared to influence the work reported in this paper.

Data availability

Data will be made available on request.

Acknowledgement

This work was supported by Universiti Kebangsaan Malaysia under Grant Code DIP-2021-003.

References

[1] Nsaif YM, Hossain Lipu MS, Ayob A, Yusof Y, Hussain A. Fault detection and protection schemes for distributed generation integrated to distribution network: challenges and suggestions. IEEE Access 2021;9:142693–717. https://doi.org/10.1109/ACCESS.2021.3121087.
[2] Elshrief YA, et al. An innovative hybrid method for islanding detection using fuzzy classifier for different circumstances including NDZ. J Radiat Res Appl Sci 2022;15(2):129–42. https://doi.org/10.1016/j.jrras.2022.04.008.
[3] Cui Q, El-Arroudi K, Joos G. Islanding detection of hybrid distributed generation under reduced non-detection zone. IEEE Trans Smart Grid 2018;9(5):5027–37. https://doi.org/10.1109/TSG.2017.2679101.
[4] Shi K, Ye H, Xu P, Yang Y, Blaabjerg F. An islanding detection based on droop characteristic for virtual synchronous generator. Int J Electr Power Energy Syst 2020;123:106277. https://doi.org/10.1016/j.ijepes.2020.106277.
[5] Paiva SC, Ribeiro RL de A, Alves DK, Costa FB, Rocha T de OA. A wavelet-based hybrid islanding detection system applied for distributed generators interconnected to AC microgrids. Int J Electr Power Energy Syst 2020;121:1–10. https://doi.org/10.1016/j.ijepes.2020.106032.
[6] Shahryari E, Nooshyar M, Sobhani B. Combination of neural network and wavelet transform for islanding detection of distributed generation in a small-scale network. Int J Ambient Energy 2019;40(3):263–73. https://doi.org/10.1080/01430750.2017.1392348.
[7] Laghari JA, Mokhlis H, Karimi M, Bakar AHA, Mohamad H. An islanding detection strategy for distribution network connected with hybrid DG resources. Renew Sustain Energy Rev 2015;45:662–76. https://doi.org/10.1016/j.rser.2015.02.037.
[8] Kim M-S, Haider R, Cho G-J, Kim C-H, Won C-Y, Chai J-S. Comprehensive review of islanding detection methods for distributed generation systems. Energies 2019;12(5):837–58. https://doi.org/10.3390/en12050837.
[9] Radhakrishnan RM, Sankar A, Rajan S. Synchrophasor based islanding detection for microgrids using moving window principal component analysis and extended mathematical morphology. IET Renew Power Gener 2020;14(12):2089–99. https://doi.org/10.1049/iet-rpg.2019.1240.
[10] Subramanian K, Loganathan AK. Islanding detection using a micro-synchrophasor for distribution systems with distributed generation. Energies 2020;13(19):5180–211. https://doi.org/10.3390/en13195180.
[11] Katyara S, et al. Wireless networks for voltage stability analysis and anti-islanding protection of smart grid system. Wirel Pers Commun 2021;116(2):1361–78. https://doi.org/10.1007/s11277-020-07432-w.
[12] Chafi ZS, Afrakhte H, Borghetti A. μPMU-based islanding detection method in power distribution systems. Int J Electr Power Energy Syst 2023;151:109102. https://doi.org/10.1016/j.ijepes.2023.109102.
[13] Shukla A, Dutta S, Sadhu PK. An island detection approach by μ-PMU with reduced chances of cyber attack. Int J Electr Power Energy Syst 2021;126:1–12. https://doi.org/10.1016/j.ijepes.2020.106599.
[14] Liu M, Zhao W, Wang Q, Huang S, Shi K. An irregular current injection islanding detection method based on an improved impedance measurement scheme. Energies 2018;11(9):2474–92. https://doi.org/10.3390/en11092474.
[15] Kaewthai S, Ekkaravarodome C, Jirasereeamornkul K. Novel disturbance and observation based active islanding detection for three-phase grid-connected inverters. J Power Electron 2021;21(2):438–50. https://doi.org/10.1007/s43236-020-00195-4.
[16] Murugesan S, Murali V. Hybrid analyzing technique based active islanding detection for multiple DGs. IEEE Trans Ind Informatics 2019;15(3):1311–20. https://doi.org/10.1109/TII.2018.2846025.
[17] Sivadas D, Vasudevan K. An active islanding detection strategy with zero nondetection zone for operation in single and multiple inverter mode using GPS synchronized pattern. IEEE Trans Ind Electron 2020;67(7):5554–64. https://doi.org/10.1109/TIE.2019.2931231.
[18] Llonch-Masachs M, Heredero-Peris D, Chillón-Antón C, Montesinos-Miracle D, Villafáfila-Robles R. Impedance measurement and detection frequency bandwidth, a valid island detection proposal for voltage controlled inverters. Appl Sci 2019;9(6):1–22. https://doi.org/10.3390/app9061146.
[19] Nale R, Biswal M, Kishor N. A transient component based approach for islanding detection in distributed generation. IEEE Trans Sustain Energy 2019;10(3):1129–38. https://doi.org/10.1109/TSTE.2018.2861883.
[20] Abo-Khalil AG, Eltamaly AM, Alharbi W, Al-Qawasmi A, Alobaid M, Alarifi IM. A modified active frequency islanding detection method based on load frequency and chopping fraction changes. Int Trans Electr Energy Syst 2021;31(11):Nov. https://doi.org/10.1002/2050-7038.13033.
[21] Dmitruk K, Sikorski A. Implementation of the improved active frequency drift anti-islanding method into the three-phase AC/DC converter with the LCL grid filter. Energies 2022;15(4):1323. https://doi.org/10.3390/en15041323.
[22] Tajdinian M, Khosravi H, Samet H, Ali ZM. Islanding detection scheme using potential energy function based criterion. Electr Power Syst Res 2022;209:1–25. https://doi.org/10.1016/j.epsr.2022.108047.
[23] Zamani R, Hamedani Golshan ME, Haes Alhelou H, Hatziargyriou N. A novel hybrid islanding detection method using dynamic characteristics of synchronous generator and signal processing technique. Electr. Power Syst. Res. 2019;175. https://doi.org/10.1016/j.epsr.2019.105911.
[24] Shrivastava S, Jain S, Nema RK, Chaurasia V. Two level islanding detection method for distributed generators in distribution networks. Int J Electr Power Energy Syst 2017;87:222–31. https://doi.org/10.1016/j.ijepes.2016.10.009.
[25] Bakhshi-Jafarabadi R, Sadeh J, Chavez J de J, Popov M. Two-level islanding detection method for grid-connected photovoltaic system-based microgrid with small non-detection zone. IEEE Trans. Smart Grid, Mar. 2021;12(2):1063–72. https://doi.org/10.1109/TSG.2020.3035126.
[26] Serrano-Fontova A, Bakhshi-Jafarabadi R. A new hybrid islanding detection method for mini hydro-based microgrids. Int J Electr Power Energy Syst 2022;143:108437. https://doi.org/10.1016/j.ijepes.2022.108437.
[27] Mlakic D, Baghaee HR, Nikolovski S. A novel ANFIS-based islanding detection for inverter-interfaced microgrids. IEEE Trans Smart Grid 2019;10(4):4411–24. https://doi.org/10.1109/TSG.2018.2859360.
[28] Shahryari E, Nooshyar M, Sobhani B. Combination of neural network and wavelet transform for islanding detection of distributed generation in a small-scale network. Int J Ambient Energy 2019;40(3):263–73. https://doi.org/10.1080/01430750.2017.1392348.
[29] Sadoughi M, Hojjat M, Hosseini Abardeh M. Detection of islanding, operation and reconnection of microgrids to utility grid using local information. Int Trans Electr Energy Syst 2020;30(8):1–19. https://doi.org/10.1002/2050-7038.12472.
[30] Baghaee HR, Mlakic D, Nikolovski S, Dragicevic T. Anti-islanding protection of PV-based microgrids consisting of PHEVs using SVMs. IEEE Trans Smart Grid 2020;11(1):483–500. https://doi.org/10.1109/TSG.2019.2924290.
[31] Allan OA, Morsi WG. A new passive islanding detection approach using wavelets and deep learning for grid-connected photovoltaic systems. Electr Power Syst Res 2021;199:1–11. https://doi.org/10.1016/j.epsr.2021.107437.
[32] Sarangi S, Sahu BK, Rout PK. Detection and classification of islanding by using variational mode decomposition and adaptive multi-kernel based extreme learning machine technique. Sustain Energy, Grids Networks 2022;30:100668. https://doi.org/10.1016/j.segan.2022.100668.
[33] Nsaif YM, Hossain Lipu MS, Hussain A, Ayob A, Yusof Y, Zainuri MAAM. A Novel fault detection and classification strategy for photovoltaic distribution network using improved hilbert-huang transform and ensemble learning technique. Sustainability 2022;14(18):11749. https://doi.org/10.3390/su141811749.
[34] Nsaif YM, Hossain Lipu MS, Hussain A, Ayob A, Yusof Y, Zainuri MAAM. A new voltage based fault detection technique for distribution network connected to photovoltaic sources using variational mode decomposition integrated ensemble bagged trees approach. Energies 2022;15(20). doi: 10.3390/en15207762.
[35] Dhibi K, Mansouri M, Bouzrara K, Nounou H, Nounou M. An enhanced ensemble learning-based fault detection and diagnosis for grid-connected PV systems. IEEE Access 2021;9:155622–33. https://doi.org/10.1109/ACCESS.2021.3128749.
[36] Laghari JA, Mokhlis H, Bakar AHA, Karimi M. A new islanding detection technique for multiple mini hydro based on rate of change of reactive power and load connecting strategy. Energy Convers Manag 2013;76:215–24. https://doi.org/10.1016/j.enconman.2013.07.033.
[37] Jhuma UK, Ahmad S, Ahmed T. A novel approach for secure hybrid islanding detection considering the dynamic behavior of power and load in electrical distribution networks. Sustainability 2022;14(19):12821. https://doi.org/10.3390/su141912821.

[38] Song G, Cao B, Chang L. A passive islanding detection method for distribution power systems with multiple inverters. IEEE J Emerg Sel Top Power Electron Oct. 2022;10(5):5727–37. https://doi.org/10.1109/JESTPE.2022.3165631.
[39] Nale R, Biswal M, Kishor N. A passive communication based islanding detection technique for AC microgrid. Int J Electr Power Energy Syst 2022;137:1–12. https://doi.org/10.1016/j.ijepes.2021.107657.
[40] Sawas AM, Woon WL, Pandi R, Shaaban M, Zeineldin H. A multistage passive islanding detection method for synchronous-based distributed generation. IEEE Trans Ind Inform 2022;18(3):2078–88. https://doi.org/10.1109/TII.2021.3065015.